

# Compressive Strength and Microstructural Characteristics of Natural Zeolite-Based Geopolymer

62(1), pp. 64–71, 2018

<https://doi.org/10.3311/PPci.10848>

Creative Commons Attribution 

Sevgi Özen<sup>1\*</sup>, Burhan Alam<sup>2</sup>

RESEARCH ARTICLE

Received 05 April 2017; Revised 17 May 2017; Accepted 24 May 2017

## Abstract

*A detailed study of geopolymeric reaction products and mechanical properties of geopolymer pastes prepared with natural zeolite has been investigated by means of compressive strength, XRD and SEM/EDX analysis. Sodium silicate and sodium hydroxide solutions are used as an alkaline activator. The results of the investigation show that the activator ratio plays an important role on the mechanical development of geopolymer pastes. The geopolymeric gel and CSH phase with a low Ca/Si ratio are found as the main reaction product. The increased intensity of CSH phase has a significant effect on the improvement of the compressive strength. Decreased intensity of clinoptilolite and totally consumed clay mineral upon geopolymerization proves the involvement of the aluminosilicate phases in the geopolymeric reaction. The existence of sodium and increment of Si/Al ratio with respect to original zeolitic tuff were detected. The results also show that the investigated natural zeolite, which is emerged as an environmentally friendly, low-cost material, is suitable for the production of geopolymer cement.*

## Keywords

*natural zeolite, geopolymer, compressive strength, microstructural characteristics*

## 1 Introduction

The manufacturing of Portland cement causes CO<sub>2</sub> emission through the calcination of the raw materials during clinker production. One ton of Portland cement production results in the release of approximately one ton of CO<sub>2</sub> emissions into the atmosphere. Global CO<sub>2</sub> emission from cement production is now 5–8% and it is estimated to be about 17% in a few years due to the fast growing industry [1]. The development of new binding materials with low CO<sub>2</sub> impact is essential for future global warming solutions since many scientists predict that level of CO<sub>2</sub> in the atmosphere already go beyond the safe limit [2].

Blended cements obtained by mixing Portland cement with mineral admixtures are widely used in building industry in order to reduce the use of Portland cement. The use of such materials may lead not only to a significant reduction in CO<sub>2</sub> emission but also to an improvement in workability and sulphate resistance, low-cost, reduced energy consumption, lower heat of hydration, enhanced long-term mechanical strength and so on [3–11]. Nevertheless, there are some disadvantage of using blended cement. The main one in general is that they have an early strength development lower than Portland cement [4,12,13]. Besides, only a portion of the cement in concrete is replaced by supplementary cementing materials.

Nowadays, new binding material seen as an alternative to Portland cement is being developed. This new technology could release 80–90% less CO<sub>2</sub> emission related to the manufacturing of cement, while at the same time it provides high early strength, freeze-thaw resistance, corrosion resistance and sulphate resistance [14,15]. This new cementitious system is called “geopolymer” after Davidovits [16]. Although there are abundance of names used to describe these new materials, referring geopolymer [16], low-temperature aluminosilicate glass [17], alkali-activated cement [18], hydroceramic [19], alkali-bonded ceramic [20] and inorganic polymer [21], they all designate the same mechanism, which involves an alkali activation of natural or artificial aluminosilicate materials such as fly ash [22,23,24,25], blast furnace slag [26,27], kaoline [28] and natural pozzolans [29,30].

<sup>1</sup>Industrial Design Engineering,  
Faculty of Engineering,  
Recep Tayyip Erdogan University  
53100 Fener-Rize, Turkey

<sup>2</sup>Civil Engineering Department,  
Faculty of Engineering,  
Middle East Technical University,  
06000 Ankara, Turkey

\*Corresponding author, email: [sevgi.ozen@erdogan.edu.tr](mailto:sevgi.ozen@erdogan.edu.tr)

As a natural pozzolan, zeolite provides an important opportunity to be used as geopolymer cement due to its natural, low-cost and widespread occurrences in worldwide. However, the studies on the synthesis of geopolymer by the alkali-activation of natural zeolites are limited [31,32]. The majority of published papers on natural zeolite-based geopolymers have focused on the effect of variables. In general the methods of analysis have been limited to investigation of compressive strength analysis [32,33,34]. Meantime, microstructural characteristics of resulting products has been less intensely examined [31]. Further research is required to explore geopolymeric reaction products of zeolite-based binding material. Therefore the present work is aimed to gaining better understanding of geopolymeric reaction products and mechanical properties of geopolymer pastes prepared with natural zeolite by analyzing the resulting geopolymers with the aid of compressive strength, XRD and SEM/EDX analysis.

## 2 Experimental

### 2.1 Materials, synthesis and mixing procedure

The zeolite-rich tuff used in the study was obtained from a natural deposit in Gördes, Turkey. The samples were ground by using a ball mill, and a fine material with an average surface of 3500 cm<sup>2</sup>/g was obtained. Sodium silicate solution (Na<sub>2</sub>O = 9.8%, SiO<sub>2</sub> = 27.7% and water = 62.5% by mass) and analytical grade sodium hydroxide (12M) were used as the alkaline activators. The sodium hydroxide solution was prepared by dissolving sodium hydroxide flakes with 98 purity in distilled water.

The zeolite bearing tuff and NaOH solution were first mixed in a Hobart mixer for 2 to 3 minutes. Sodium silicate was then added and mixed for 3 to 5 minutes. Tuff/activator ratio of 1.75 and sodium silicate/sodium hydroxide ratios of 1, 2 and 3 were used. After the mixing procedure is done, the fresh geopolymer paste was cast in 50×50×50 mm cube mold as described in ASTM C109. The specimens were removed from the molds and covered by a film to prevent the loss of moisture. The specimens were then cured at 25°C, 50°C and 75°C for 7, 28, 56 days.

### 2.2 Methods

The chemical composition of zeolite-rich tuff was determined using X-ray fluorescence analysis (XRF, Rigaku ZSX Primus II). The particle size distribution analysis was performed by using Malvern Mastersizer 2000 laser particle size analyzer. The compressive strengths of zeolite-based geopolymer specimens were measured after 7, 28 and 56 days of curing in accordance with ASTM C109 using a universal testing machine at a loading rate of 1 kNs<sup>-1</sup>. The strength values were obtained from the average of three measurements for each sample. The mineralogical characteristics of untreated tuff and zeolite-based geopolymer pastes were examined with X-ray diffraction (XRD) analysis (after crushing and sieving the samples to obtain particles smaller than 63µm) by using Philips PW 1730 diffractometer

with Ni-filtered, CuKα1 radiation, operating at 40 kV, 30 mA. Scanning electron microscope (SEM) using a QUANTA 400F device, equipped with energy-dispersive X-ray (EDX) system, was employed to observe the morphology and microstructure of original zeolite-rich tuff and zeolite-based geopolymer pastes. EDX was used to analyse semi-quantitative elemental composition of the surface of a specimen. The samples were coated with carbon before SEM-EDX analysis. XRD and SEM/EDX analysis were performed on the three sample representing the highest, the lowest, and the middle strength values and measurements were performed on the hardened pastes testing the compressive strength analysis.

## 3 Results and Discussion

### 3.1 Characteristics of zeolite bearing tuffs

The chemical composition of the zeolite-rich tuff is given in Table 1. The total SiO<sub>2</sub> and Al<sub>2</sub>O<sub>3</sub> content, which are the main constituents of the geopolymeric reaction, is 78.8% and it is within the range of values reported by Davidovits (1994) [30]. In Fig. 1, the grain size distribution of ground zeolite-bearing tuff is presented.

**Table 1** Chemical composition of zeolite-rich tuff

Component	Weight (%)
SiO <sub>2</sub>	65.6
Al <sub>2</sub> O <sub>3</sub>	13.2
Fe <sub>2</sub> O <sub>3</sub>	1.78
CaO	4.43
MgO	1.27
Na <sub>2</sub> O	0.21
K <sub>2</sub> O	2.8
SO <sub>3</sub>	0.07
MnO	0.05
LOI	10.32
<b>Total</b>	<b>99.73</b>

Mineral phases of the zeolite bearing tuff are shown in Fig. 2. According to the XRD pattern, clinoptilolite is the major component (2θ of 9.83, 11.16, 22.36 with *d*-spacing values of 8.99, 7.93, 3.98 Å, respectively). Minor amount of quartz is identified with *d*-spacing values of 3.34 and 4.26 Å. A peak identified with *d*-spacing values of 10.01 and 2.58 Å due to presence of clay mineral (illite) is also presented in the XRD pattern.

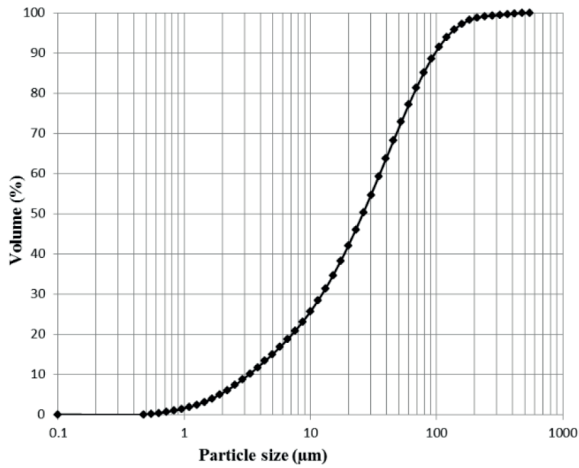


Fig. 1 Grain size distribution of zeolitic tuff sample

Fig. 3 displays the microstructure and morphology of the original zeolite-rich tuff before grinding. As seen in the figure, clinoptilolites have characteristic morphology of tabular plates and laths, some of which have coffin-shaped crystals [35]. The point studied of pindicates site where semi-quantitative chemical analysis by EDX was conducted and results are presented in Table 2. According to EDX measurement, the Si/Al ratio of the original clinoptilolite was found to be 4.78 (Table 2).

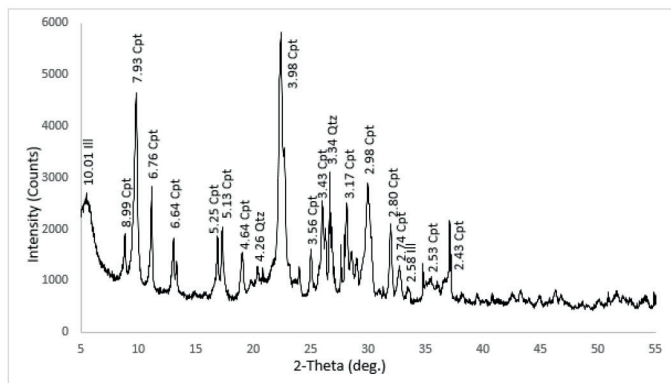


Fig. 2 XRD pattern of zeolitic tuff (Ill: illite, Cpt: clinoptilolite, Qtz: quartz)

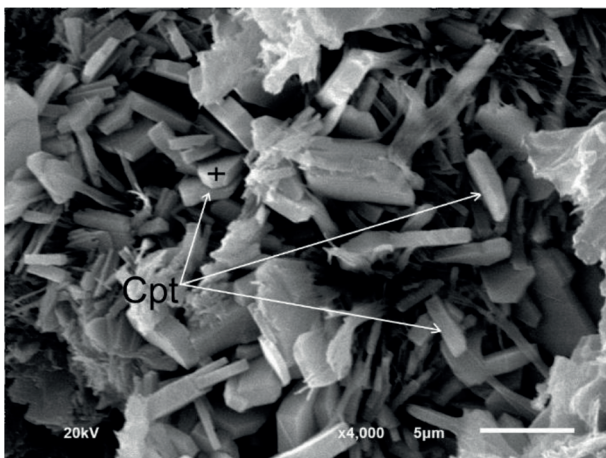


Fig. 3 SEM micrograph shows clinoptilolite crystals displaying laths and tabular plates (Cpt: clinoptilolite)

Table 2 Chemical analysis of original clinoptilolite determined by EDX analysis (Position of measurement is shown in Fig 3)

	Si	Al	Mg	K	Ca	C	O	Si/Al	Sum
1	33.06	6.91	1.03	1.79	2.08	7.96	47.17	4.78	100

### 3.2 Compressive Strength

Fig. 4 shows the compressive strength of the natural zeolite based geopolymers at three different  $\text{Na}_2\text{SiO}_3/\text{NaOH}$  ratios as a function of curing temperature and time.

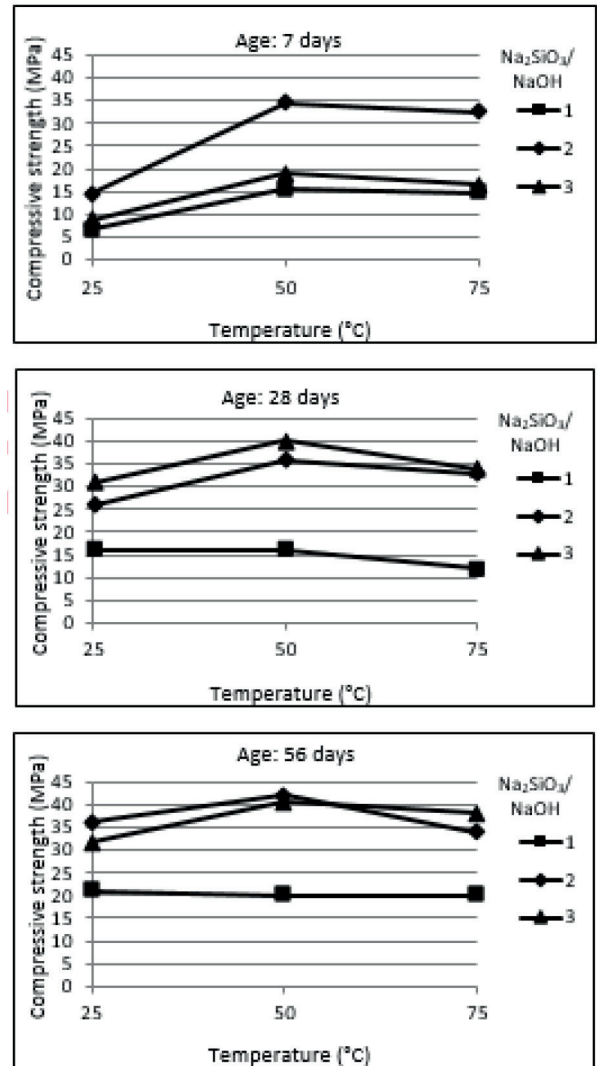


Fig. 4 Compressive strength of zeolite-rich tuff activated with different activator ratios, curing temperature and time

As seen in Fig. 4, activator ratio clearly affects the compressive strength of geopolymers. Regardless of the curing temperature and time, the  $\text{Na}_2\text{SiO}_3/\text{NaOH}$  ratio of 1 displays the lowest strength development in the tests due to the insufficient dissolution of silica and alumina from aluminosilicate source for the geopolymeric reaction to take place and thus inadequate amount of geopolymeric reaction product. The increment in the activator ratio from 1 to 2 resulted in a significant increase in the mechanical strength development of alkali-activated zeolites. The compressive strength of geopolymers with  $\text{Na}_2\text{SiO}_3/\text{NaOH}$  ratios of 2 and 3 exhibits nearly the same behavior except for

the 7 days curing. These geopolymers have good mechanical strengths, which is able to fulfil the strength requirement of typical construction materials for performance applications (25–40 MPa). The maximum compressive strength (42 MPa) was obtained for geopolymer cured at 50°C for 56 days with a  $\text{Na}_2\text{SiO}_3/\text{NaOH}$  ratio of 2.

Generally, increasing the temperature causes the reaction to proceed to a higher extent [36]. The analytical results similarly show that an increase in curing temperature from 25°C to 50°C increased the compressive strength, as seen in Fig. 4. When the temperature reached above 50°C, the strength started to decrease. However, the reactivity of geopolymer with  $\text{Na}_2\text{SiO}_3/\text{NaOH}$  ratio of 1 is not improved by heat treatment and it exhibits lower compressive strengths for all curing temperatures. The influence of temperature, thus, can be seen on geopolymer samples only having activator ratio higher than 1 in this study. In other words, it can be said that the effect of temperature can be observed with suitable activator ratio.

It is also worth noting that at room temperature long curing is necessary for mechanical development. For alkali-activated samples cured at 50°C, however, an important increase was observed at the first week of curing. The main reason of the quick strength gain is the increased reactivity between silica and alumina resulted from higher temperature. Consequently, higher curing temperatures can be used when rapid strength development is needed in a short period of time [37].

### 3.3 Microstructural Characteristics

#### 3.3.1 XRD

X-ray diffraction patterns of raw zeolitic tuff and hardened geopolymer pastes with highest, the lowest, and the middle strength values are shown in Fig. 5.

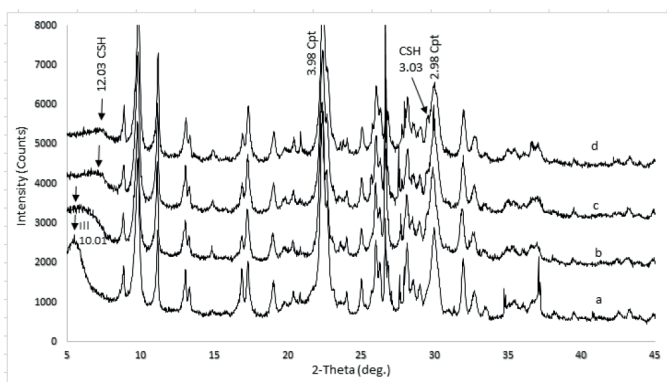


**Fig. 5** XRD patterns of a) original zeolite-rich tuff, b) geopolymer paste for  $\text{Na}_2\text{SiO}_3/\text{NaOH}$  ratio of 1 cured at 25°C and 7 days; c) for  $\text{Na}_2\text{SiO}_3/\text{NaOH}$  ratio of 2 cured at 25°C and 28 days; d) for  $\text{Na}_2\text{SiO}_3/\text{NaOH}$  ratio of 2 cured at 50°C and 56 days (Ill: illite, Cpt: clinoptilolite, CSH: calcium silicate hydrate)

The XRD pattern of geopolymer with  $\text{Na}_2\text{SiO}_3/\text{NaOH}$  ratio of 1 cured at 25°C for 7 days is almost similar to that of raw zeolite rich tuff (clinoptilolite, quartz, clay mineral) and new crystalline phases were not detected (Fig. 5b). Peak of clay and zeolite minerals were still observed in the diffractogram with

decreased intensity. Furthermore, the broad band at  $2\theta$  between 25° and 35°, typical amorphous phase of geopolymer gel, was detected [29]. This indications apparently suggest that the geopolymeric reaction start to reorganize the structure of the system. The slightly reduced peak intensities, however, indicate that reactive component found in tuff (clinoptilolite and clay mineral) do not fully attend the reaction and the formation of geopolymeric reaction product which give the strength ability is small. This observation was confirmed by compressive strength analysis, which is only 6.7 MPa for geopolymer with  $\text{Na}_2\text{SiO}_3/\text{NaOH}$  ratio of 1 cured at 25°C for 7 days (Fig. 4).

The peak observed with d-spacing value of 10.01, which correspond to illite in raw clinoptilolite-rich tuff, totally disappeared and new crystalline phases are detected at higher activator concentration (Fig. 5c). The peak at 12.03 (d-spacing) and shoulder at 3.03 identified to the left of the peak at 2.98 (d-spacing) started to be seen for geopolymer with  $\text{Na}_2\text{SiO}_3/\text{NaOH}$  ratio of 2 cured at 25°C for 28 days. These correspond to the two main peaks of the CSH phase. CSH is normally accepted to be the main hydration product of Portland cement [38]. On the other hand, it was reported that CSH can be formed resulting from the alkaline activation of aluminosilicate source rich in calcium such as blast furnace slag [39,40]. It was demonstrated that the possible reaction products (e.g. geopolymeric gel, CSH, calcium aluminosilicate) formed if sufficient calcium is added to a geopolymeric system [39]. In this study, although a small amount of calcium content found in raw zeolitic tuff (8%), CSH peaks were determined by XRD analysis. The presence of sodium silicate in alkaline activator also might have affected the geopolymeric system and caused the formation of CSH phase. This data is in agreement with SEM/EDX micrograph (Fig. 7), which display thin CSH coating observed in pores. The compressive strength of this hardened geopolymer (26 MPa) is higher than that of geopolymer with  $\text{Na}_2\text{SiO}_3/\text{NaOH}$  ratio of 1 cured at 25°C for 7 days (6.7 MPa). A higher activator concentration has better ability to dissolve raw material, allowing a higher Si, Al species to take place in geopolymeric reaction and consequently better mechanical development.

Fig. 5d presents the XRD patterns of geopolymer paste with  $\text{Na}_2\text{SiO}_3/\text{NaOH}$  ratio of 2, 50°C at 56 days. The intensities of CSH peaks at 12.03 and 3.03 (d-spacings) are comparatively higher than those of CSH peaks for geopolymer with  $\text{Na}_2\text{SiO}_3/\text{NaOH}$  ratio of 2 cured at 25°C for 28 days. Similarly, the compressive strength of geopolymer with  $\text{Na}_2\text{SiO}_3/\text{NaOH}$  ratio of 2, 50°C at 56 days is the highest (42 MPa). As a result of this knowledge, it was assumed that the differences in the intensities of CSH peaks effect the compressive strength results.

The compressive strength is getting increased with the increased intensity of CSH peaks. Therefore, it can be said that in addition to the geopolymeric gel, the more crystalline CSH phase is beneficial to the compressive strength development of the hardened geopolymer paste.

Even though decrease in intensity of the clinoptilolite peak at 3.98 (d-spacing) was observed for all geopolymer paste, which is associated with the alteration of clinoptilolite crystal by geopolymerization, the existence of remaining clinoptilolite as a result of incomplete reaction was detected. The peak corresponding to quartz, on the other hand, was not evidently reduced [41].

### 3.3.2 SEM/EDX

SEM/EDX analyses were performed with the aim of exhibiting the phase characterization and microstructural evolution of geopolymer pastes.

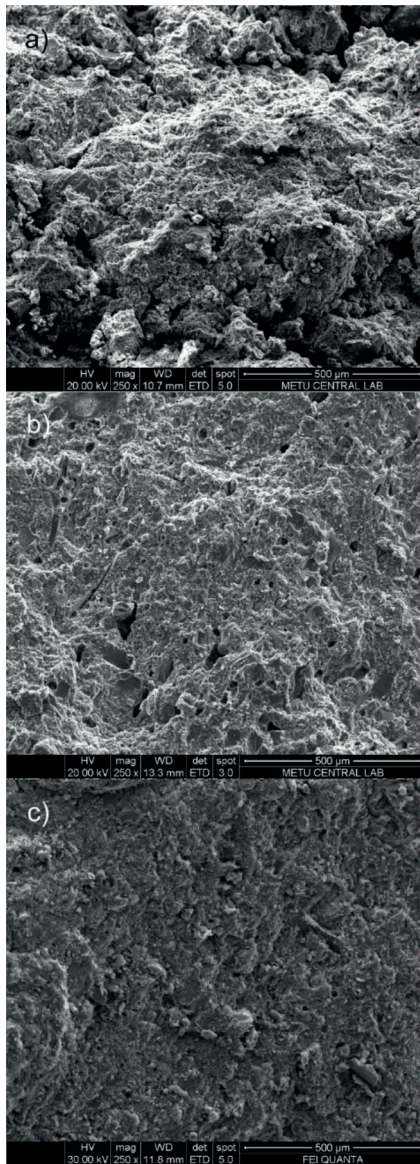


**Fig. 6** SEM micrographs of geopolymer pastes a) for  $\text{Na}_2\text{SiO}_3/\text{NaOH}$  ratio of 1, 25°C at 7 days; b) for  $\text{Na}_2\text{SiO}_3/\text{NaOH}$  ratio of 2, 25°C at 28 days; c) for  $\text{Na}_2\text{SiO}_3/\text{NaOH}$  ratio of 2, 50°C at 56 days

A general microstructural features of the hardened geopolymer pastes with the highest, the lowest, and the middle strength values are seen at Fig. 6. The analysis of the microstructure of the pastes prepared with activator ratio of 1, cured for 7 days at 25 °C revealed that the matrix consists of fragmented particles

(Fig. 6a). This indicates that formation of aluminosilicate gel, which is a main geopolymer product, was not sufficient, which is in agreement with the mechanical behavior of the same paste. Fig. 6b, however, display more compact texture, yet porous, which can decrease the compressive strength (activator ratio of 2, cured for 28 days at 25°C). As seen in Fig. 6c, the morphology of the geopolymer paste at activator ratio of 2, cured for 56 days at 50 °C is obviously different from the previously described pastes. In this case, the studied sample contains very dense material with almost no pores.

At higher magnification, three different phases were determined through morphological observations and compositional analysis by SEM and EDX as shown in Fig. 7 and Table 3. From Fig. 7a, it can be seen that the presence of some coating on the cavity surfaces. Morphologically, this phase resembles with the CSH phase as produced from Portland cement hydration. It is stated that CSH is similar to that formed from the hydration of Portland cement but with lower Ca/Si atomic ratios (0.6-1.0) (Fernandez-Jimenez et al., 2003). In this study, Ca/Si ratio of CSH coatings for geopolymer paste with  $\text{Na}_2\text{SiO}_3/\text{NaOH}$  ratio of 2, 50°C at 56 days is not higher than 0.22 (Fig. 7b). However, it must be remembered that semi-quantitative EDX analysis is likely to represent approximate elemental distributions of the phases not a reliable indicator of exact compositions.

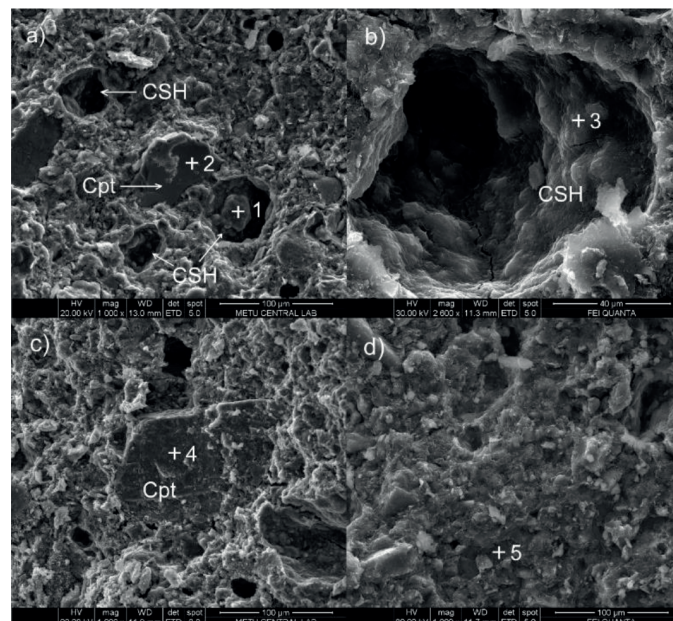


**Fig. 7** SEM/EDX analysis of geopolymer pastes a) for  $\text{Na}_2\text{SiO}_3/\text{NaOH}$  ratio of 2, 25°C at 28 days; b) for  $\text{Na}_2\text{SiO}_3/\text{NaOH}$  ratio of 2, 50°C at 56 days; c) for  $\text{Na}_2\text{SiO}_3/\text{NaOH}$  ratio of 2, 50°C at 56 days; d) for  $\text{Na}_2\text{SiO}_3/\text{NaOH}$  ratio of 2, 50°C at 56 days (CSH: calcium silicate hydrate, Cpt: clinoptilolite)

In the Fig. 7a, one can clearly distinguish a partially reacted zeolitic tuff fragment embedded within the geopolymeric paste, which is attacked by the alkaline solution during geopolymerization. The Si/Al ratio of the original zeolite-bearing tuff is 4.78, however, it changes to 1.5 in the partially reacted zeolitic tuff as a result of dissolution of zeolite (Table 3). Fig. 7c shows

the more reacted sample as a consequence of the higher alkali activation. Due to the alkaline attack, the surface texture of zeolite bearing tuff appear to be more reacted without altering their overall structure. The less reacted sample contain high Si/Al ratio, 1.5, compared with the more reacted zeolitic tuff fragments where the Si/Al ratio is 1.28.

Glass like geopolymer gel, which appears to surround and adhere to the partially reacted zeolitic tuff fragments is considered to be the third phase (Fig. 7). Microstructural investigations through EDX analyses display that glassy matrix consists mainly of Na, Al and Si, which is the essential constituent of geopolymer gel. According to elemental analysis, the Si/Al ratio in the geopolymeric matrix is 6.46 (Table 3).

Fig. 8 shows the morphology of the fracture surface of the geopolymer pastes and semi-quantitative chemical compositions of the reaction products with the lowest (Figure 8a), the middle (Figure 8b), and the highest (Figure 8c) strength values. The plots were taken from main matrix area (Table 3). The presence of Na and an increase of Si/Al ratio due to the involvement of activators reveals significant degree of geopolymeric reaction as indicated by increasing mechanical development.

#### 4 Conclusions

In this study, mechanical properties and microstructural characteristics of natural zeolite-based geopolymers were investigated.

Taking into account the results of strength analysis, it can be conclude that the compressive strength of activated natural zeolite depends on a combination of parameters. However, activator ratio is the most important parameter that significantly influences the geopolymeric reaction.

In addition to geopolymeric gel, XRD peaks of the CSH phase with a low Ca/Si ratio were determined as main reaction product resulting from the alkaline activation of raw zeolite bearing tuff. The formation of CSH phase might have affected by Ca content in zeolite bearing tuff and promoted by the presence of sodium silicate in alkaline activator. Apparently, the more crystalline CSH phase has a positive effect on the development of compressive strength of resulted geopolymer paste as observed in XRD analysis. Decreased intensity of zeolite and totally consumed clay minerals, which demonstrate dissolution and involvement of aluminosilicate phase in the geopolymeric reaction, were determined.

SEM analysis of zeolite-based geopolymer pastes demonstrates that their microstructure is characterized by the coexistence of a CSH phase, partially reacted zeolitic tuff and glassy matrix. It can be accepted that pores within the geopolymeric pastes become covered with the CSH phase. From the EDX analysis, sodium incorporation and increment of Si/Al ratio with respect to original zeolitic tuff were detected in the aluminosilicate phase.

**Table 3** Semi-quantitative chemical analysis of geopolymer pastes at various conditions determined by EDX analysis (Positions of measurements are shown in Fig. 7, 8)

	1	2	3	4	5	6	7	8
Si	41.31	22.84	37.61	24.72	43.8	35.24	40.36	46.04
Al	5.04	15.25	4.37	19.34	6.78	6.49	7.04	6.82
Fe	2.5	1.91	0.37	1.1	1.33	0.69	1.39	0.51
Mg	0	1.34	0.27	0.48	0.66	0.77	0.92	0
K	3	6.64	1.96	8.76	3.03	1.71	2.03	2.96
Ca	8.08	0.29	8.44	0.42	3.72	1.87	3.05	2.72
Na	4.1	0.38	4.15	0.87	4.16	4.98	5.28	3.89
C	6.43	4.17	7.33	4.06	4.66	4.3	3.32	4.26
O	29.54	47.18	35.5	40.25	31.86	43.94	36.61	32.79
Sum	100	100	100	100	100	100	100	100
Si/Al	8.2	1.5	8.61	1.28	6.46	5.43	5.73	6.75
Ca/Si	0.2	0.01	0.22	0.02	0.08	0.05	0.08	0.06

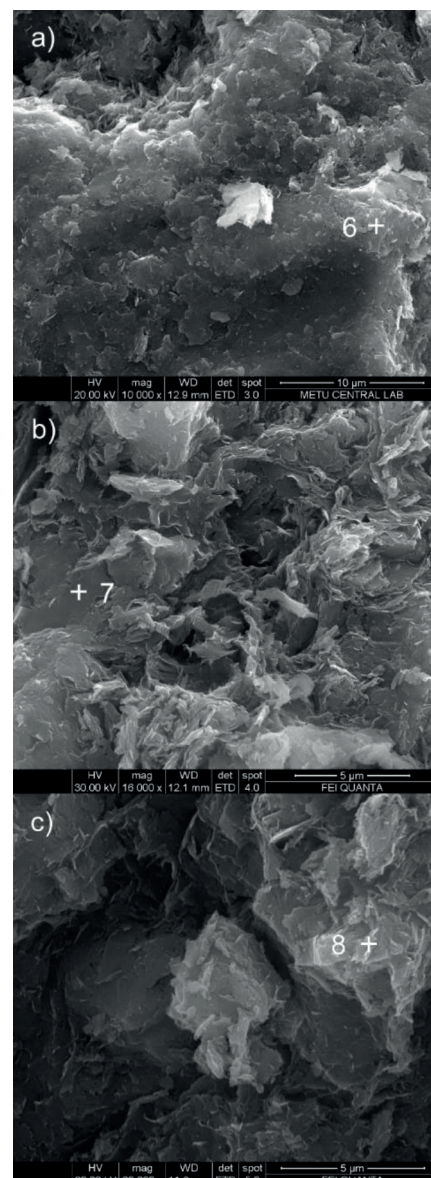


**Fig. 8** SEM/EDX analysis of geopolymer pastes a) for  $\text{Na}_2\text{SiO}_3/\text{NaOH}$  ratio of 1, 25°C at 7 days; b) for  $\text{Na}_2\text{SiO}_3/\text{NaOH}$  ratio of 2, 25°C at 28 days; c) for  $\text{Na}_2\text{SiO}_3/\text{NaOH}$  ratio of 2, 50°C at 56 days

## Acknowledgement

The investigations were carried out in the Civil Engineering Department, Middle East Technical University, Turkey. Thanks are due to Rota Mining Corporation for the contribution of sample takes from Gördes Region.

## References

- [1] Scrivener, K. L., Kirkpatrick, R. J. "Innovation in use and research on cementitious material". *Cement and Concrete Research*, 38(2), pp.128–136. 2008. <https://doi.org/10.1016/j.cemconres.2007.09.025>
- [2] Richardson, K., Steffen, W., Schellnhuber, H. J., Alcamo, J., Barker, T., Kammen, D. M., Leemans, R., Liverman, D., Munasinghe, M., Osman-Elasha, B., Stern, N., & Waever, O. "Synthesis report from climate change: Global risks, Challenges and Decisions". University of Copenhagen. Denmark. 2009. <https://www.pik-potsdam.de/news/press-releases/files/synthesis-report-web.pdf>
- [3] Shi, C. "Pozzolanic reaction and microstructure of chemical activated lime-flyash pastes". *ACI Materials Journal*, 95(5), pp. 537–545. 1998.
- [4] Mehta, P. K., Monteiro, P. J. M. "Concrete: Microstructure, Properties and Materials". McGraw-Hill. 2006.
- [5] Siddique, R., Khan, M.I. "Supplementary Cementing Material". Springer Heidelberg Dordrecht. London. 2011.
- [6] Ramezani-pour, A. A. "Cement Replacement Materials: Properties, Durability, Sustainability". Heidelberg Springer. 2014. <https://doi.org/10.1007/978-3-642-36721-2>
- [7] Cook, D. J. "Natural pozzolanas". In: *Cement Replacement Materials*, (Swamy R.N. (Ed.)). Surrey University Press. p. 200. 1986.
- [8] Rojas, M. F., Cabrera J. "The effect of temperature on the hydration rate and stability of the hydration phases of metakaolin-lime-water systems". *Cement and Concrete Research*, 32(1), pp. 133–138. 2002. [https://doi.org/10.1016/S0008-8846\(01\)00642-1](https://doi.org/10.1016/S0008-8846(01)00642-1)
- [9] Janotka, I., Krajčí L. "Utilization of natural zeolite in Portland cement of increased sulphate resistance". *ACI Special Publications*, 192, pp. 223–229. 2000.
- [10] Urrutia, C., Ubilla, M., Bobadilla, M. "Activity and properties of pozzolan used in blended cements". In: *Proceedings of the 9<sup>th</sup> International Congress on the Chemistry of Cement*. (Mullik, A. K. (Ed.)). New Delhi. India. pp. 86–92. 1992.
- [11] Chindaprasirt, P., Homwuttivong, S., Sirivivatnanon, V. "Influence of fly ash fineness on strength, drying shrinkage and sulfate resistance of blended cement mortar". *Cement and Concrete Research*, 34(7), pp. 1087–1092. 2004. <https://doi.org/10.1016/j.cemconres.2003.11.021>
- [12] Li, D., Fu, X., Wu, X., Tang, M. "Durability study of steel slag cement". *Cement and Concrete Research*, 27(7), pp. 983–987. 1997. [https://doi.org/10.1016/S0008-8846\(97\)00084-7](https://doi.org/10.1016/S0008-8846(97)00084-7)
- [13] Zhu, G., Sun, S. "Current situation and trend of iron and steel slag utilization in P. R. China". In: *International Symposium on the Utilization of Metallurgical Slag*. Beijing, P.R. China. pp. 10–15. 1999.
- [14] Davidovits, J. "Carbon-Dioxide Greenhouse-Warming: What Future for Portland Cement". In: *Emerging Technologies Symposium on Cements and Concretes in the Global Environment*. Symposium 147, Chicago 1993. p.21.
- [15] Duxson, P., Lukey, G., Van Deventer, J. S. J. "Physical evolution of geopolymer derived from metakaolin up to 1000 °C". *Journal of Material Science*, 42(9), pp. 3044–3054. 2007. <https://doi.org/10.1007/s10853-006-0535-4>
- [16] Davidovits, J. "Geopolymers: inorganic polymeric new materials". *Journal of Thermal Analysis and Calorimetry*, 37(8), pp. 1633–1656. 1991. [10.1007/BF01912193](https://doi.org/10.1007/BF01912193)
- [17] Rahier, H., Van Mele, B., Biesemans, M., Wastiels, J., Wu, X. "Low-temperature synthesis of aluminosilicate glasses". *Journal of Material Science*, 31(1), pp. 71–79. 1996. <https://doi.org/10.1007/BF00355128>
- [18] Palomo, A., de la Fuente, J. I. L. "Alkali-activated cementitious materials: alternative matrices for the immobilisation of hazardous wastes. Part I. Stabilisation of boron". *Cement and Concrete Research*, 33(2), pp. 281–288. 2003. [https://doi.org/10.1016/S0008-8846\(02\)00963-8](https://doi.org/10.1016/S0008-8846(02)00963-8)
- [19] Bao, Y., Grutzeck, M. W., Jantzen, C. M. "Preparation and Properties of Hydroceramic Waste Forms Made with Simulated Hanford Low-Activity Waste". *Journal of American Ceramic Society*, 88(12), pp. 3287–3302. 2005. <https://doi.org/10.1111/j.1551-2916.2005.00775.x>
- [20] Mallicoat, S., Sarin, P., Kriven, W. M. "Novel, alkali-bonded, ceramic filtration membranes". *Ceramic Engineering and Science Proceedings*, 26, pp. 37–41. 2005. <https://doi.org/10.1002/9780470291283.ch5>
- [21] Sofi, M., Van Deventer, J. S. J., Mendis, P. A., Lukey, G. C. "Engineering Properties of Inorganic Polymer Concretes (IPCs)". *Cement and Concrete Research*, 37(2), pp. 251–257. 2007. <https://doi.org/10.1016/j.cemconres.2006.10.008>
- [22] Fernández-Jiménez, A., Palomo, A., Criado, M. "Microstructure development of alkali-activated by fly ash cement: a descriptive model". *Cement and Concrete Research*, 35(6), pp.1204–1209. 2005. <https://doi.org/10.1016/j.cemconres.2004.08.021>
- [23] Bakharev, T. "Geopolymer materials prepared using class F fly ash and elevated temperature curing". *Cement and Concrete Research*, 35(6), pp. 1224–1232. 2005. <https://doi.org/10.1016/j.cemconres.2004.06.031>
- [24] Palomo, A., Grutzeck, M. W., Blanco, M. T. "Alkali-activated fly ashes. A cement for future". *Cement and Concrete Research*, 29(8), pp. 1323–1329. 1999. [https://doi.org/10.1016/S0008-8846\(98\)00243-9](https://doi.org/10.1016/S0008-8846(98)00243-9)
- [25] Van Jaarsveld, J. G. S., Van Deventer, J. S. J., Lukey, G. C. "The Characterization of Source Materials in Fly Ash-based Geopolymers". *Materials Letters*, 57(7), pp. 1272–1280. 2003. [https://doi.org/10.1016/S0167-577X\(02\)00971-0](https://doi.org/10.1016/S0167-577X(02)00971-0)
- [26] Fernández-Jiménez, A., Palomo, J. G., Puertas, F. "Alkali-activated slag mortars mechanical strength behavior". *Cement and Concrete Research*, 29(8), pp. 1313–21. 1999. [https://doi.org/10.1016/S0008-8846\(99\)00154-4](https://doi.org/10.1016/S0008-8846(99)00154-4)
- [27] Bakharev, T., Sanjayan, J., Cheng, Y. "Sulfate attack on alkali-activated slag concrete". *Cement and Concrete Research*, 32(2), pp. 211–216. 2002. [https://doi.org/10.1016/S0008-8846\(01\)00659-7](https://doi.org/10.1016/S0008-8846(01)00659-7)
- [28] Zhang, S., Gong, K., Lu, J. "Novel modification method for inorganic geopolymer by using water soluble organic polymer". *Materials Letters*, 58(8), pp. 1292–1296. 2004. <https://doi.org/10.1016/j.matlet.2003.07.051>
- [29] Duxson, P., Provis, J. L., Lukey, G. C., Mallicoat, S. W., Kriven, W. M., Van Deventer, J. S. J. "Understanding the relationship between geopolymer composition, microstructure and mechanical properties". *Colloids and Surfaces A: Physicochemical Engineering Aspects*, 269(1–3), pp. 47–58. 2005. <http://dx.doi.org/10.1016/j.colsurfa.2005.06.060>
- [30] Davidovits, J. "Properties of geopolymer cements". In: *First International Conference on Alkaline Cements and Concretes*. Kiev. Ukraine. pp. 131–149. 1994.
- [31] Villa, C., Pecina, E. T., Torres, R., Gómez, L. "Geopolymer synthesis using alkaline activation of natural zeolite". *Construction and Building Materials*, 24(11), pp.2084–2090. 2010. <https://doi.org/10.1016/j.conbuildmat.2010.04.052>
- [32] Bondar, D., Lynsdale, C. J., Milestone, N. B., Hassani, N., Ramezani-pour, A. A. "Effect of heat treatment on reactivity-strength of alkali-activated natural pozzolans". *Construction and Building Materials*, 25(10), pp. 4065–71. 2011. <https://doi.org/10.1016/j.conbuildmat.2011.04.044>

- [33] Bondar, D , Lynsdale, C J , Milestone, N B , Hassani, N , Ramezani-pour, AA. "Effect of type, form and dosage of activatorsonstrength of alkali-activatednaturalpozzolans". *Cement and ConcreteComposite*, 33(2), pp. 251–260.2011. <https://doi.org/10.1016/j.cemconcomp.2010.10.021>
- [34] Değirmenci, F. N. "Utilization of natural and wastepozzolansas an alternativeresource of geopolymer mortar". *International Journal of Civil Engineering*, pp. 1–10. 2016. <https://doi.org/10.1007/s40999-016-0115-1>
- [35] Mumpton, F. A., Ormsby, W. C. "Morphology of zeolites in sedimentary rocks by scanning electron microscopy". In: *Natural Zeolites: Occurrence, Properties, Use*. (Sand L. B., Mumpton F.A. (Eds.)). Pergamon Press. New York. pp. 113–132. 1978.
- [36] Duxson, P., Fernandez-Jimenez, A., Provis, J. L., Lukey, G. C., Palomo, A., Van Deventer, J. S. J. "Geopolymer technology: the currentstate of the art". *Journal of Material Science*, 42(9), pp. 2917–2933. 2007. <https://doi.org/10.1007/s10853-006-0637-z>
- [37] de Vargas, A. S., dal Molin, D. C. C., Vilela, A. C. F., da Silva, F. J., Pavao, B., Veit, H. "The effects of Na<sub>2</sub>O/SiO<sub>2</sub>molar ratio, curingtemperature and ageoncompressivestrength, morphology and microstructure of alkali-activatedflyash-basedgeopolymers". *Cement and Concrete Composite*, 33(6), pp. 653–660. 2011. <https://doi.org/10.1016/j.cemconcomp.2011.03.006>
- [38] Taylor, H.F.W. "*The chemistry of cements*". Academic Press. London. 1964.
- [39] Yip, C. K., Lukey, G. C., Van Deventer, J. S. J. "The coexistence of geopolymericgel and calciumsilicatehydrateattheearlystage of alkalineactivation". *Cement and Concrete Research*, 35(9), pp. 1688–1697. 2005. <https://doi.org/10.1016/j.cemconres.2004.10.042>
- [40] Khale, D., Chaudhary, R. "Mechanism of geopolymerisation and factors influencing its development: a review". *Journal of Material Science*, 42, pp. 729–746. 2007. <https://doi.org/10.1007/s10853-006-0401-4>
- [41] Fernandez-Jimenez, A., Palomo, A. "Composition and microstructure of alkali activated fly ash binder: Effect of theactivator". *Cement and Concrete Research*, 35, pp. 1984–1992. 2005. <https://doi.org/10.1016/j.cemconres.2005.03.003>